

Evidence for oxygenic photosynthesis half a billion years before the Great Oxidation Event

Noah J. Planavsky^{1*}, Dan Asael², Axel Hofmann³, Christopher T. Reinhard⁴, Stefan V. Lalonde⁵, Andrew Knudsen⁶, Xiangli Wang^{1,7}, Frantz Ossa Ossa³, Ernesto Pecoits⁸, Albertus J. B. Smith³, Nicolas J. Beukes³, Andrey Bekker⁹, Thomas M. Johnson⁷, Kurt O. Konhauser⁸, Timothy W. Lyons⁹ and Olivier J. Rouxel²

The early Earth was characterized by the absence of oxygen in the ocean–atmosphere system, in contrast to the well-oxygenated conditions that prevail today. Atmospheric concentrations first rose to appreciable levels during the Great Oxidation Event, roughly 2.5–2.3 Gyr ago. The evolution of oxygenic photosynthesis is generally accepted to have been the ultimate cause of this rise, but it has proved difficult to constrain the timing of this evolutionary innovation^{1,2}. The oxidation of manganese in the water column requires substantial free oxygen concentrations, and thus any indication that Mn oxides were present in ancient environments would imply that oxygenic photosynthesis was ongoing. Mn oxides are not commonly preserved in ancient rocks, but there is a large fractionation of molybdenum isotopes associated with the sorption of Mo onto the Mn oxides that would be retained. Here we report Mo isotopes from rocks of the Sinqeni Formation, Pongola Supergroup, South Africa. These rocks formed no less than 2.95 Gyr ago³ in a nearshore setting. The Mo isotopic signature is consistent with interaction with Mn oxides. We therefore infer that oxygen produced through oxygenic photosynthesis began to accumulate in shallow marine settings at least half a billion years before the accumulation of significant levels of atmospheric oxygen.

Despite detailed investigations over the past 50 years, there is still intense debate about when oxygenic photosynthesis evolved^{1,4,5}. Current estimates span more than a billion years of Earth history, ranging from before 3.7 Gyr ago (Ga; ref. 6), the age of the oldest sedimentary rocks, to 2.5–2.3 Ga, coincident with the rise of atmospheric oxygen (the Great Oxidation Event, GOE; refs 7,8). Until recently, organic molecular data were regarded as undisputed evidence for cyanobacteria (and thus oxygenic photosynthesis) by at least 2.7 Ga⁵. However, given mounting evidence that the initial excitement about this biomarker work was at least premature^{4,9}, there is essentially no solid constraint on the onset of biological oxygen production. Current geochemical and biomarker evidence for the development of oxygenic photosynthesis before the GOE (2.5–2.3 Ga) is, arguably, inconclusive^{1,4}. As such, a new, independent perspective is needed. We provide such a perspective herein by using Mo isotopes in a new way to track the onset of Mn(II) (Mn²⁺) oxidation and thus biological oxygen production.

The oxidation of Mn(II) in modern marine settings requires free dissolved oxygen (O₂). Moreover, given strong kinetic inhibition,

Mn(II) oxidation in marine settings is microbially mediated^{10,11}, with most microbial Mn(II) oxidation being attributed to direct enzymatic activity¹¹. This reaction can also be catalysed by transmembrane protein-driven reduction of O₂ to the redox reactant superoxide (O₂⁻) and this pathway is also likely to be significant in natural environments^{12,13}. Where the kinetics of marine Mn oxidation have been studied in detail, O₂ concentrations exert a direct control on the rate of Mn oxidation and the reaction can be modelled with Michaelis–Menten-type kinetics¹⁴. In simple aqueous solutions, photochemical Mn oxidation under anoxic conditions is possible¹⁵; however, this process is inhibited in the presence of reductants (for example, Fe(II); ref. 15). Furthermore, the rates of this process make it unlikely to be geologically significant¹⁵. Finally, there is no evidence for environmentally significant microbial phototrophic Mn oxidation, despite intensive investigation on anoxygenic photosynthetic pathways. In this regard, Mn is rather unique in its environmental specificity for O₂ as an electron acceptor among the redox-sensitive transition metals, many of which, like Fe, can be oxidized under anoxic conditions either through a microbial pathway and/or with alternative oxidants such as NO₃⁻.

Microbial Mn oxidation in an aqueous environment requires O₂ concentrations that are orders of magnitude higher than those in gas exchange equilibrium with our best estimates for the prebiotic or Archaean atmosphere ([O₂] ≪ 10⁻⁵ present atmospheric levels¹). It is only through photosynthetic water splitting that free oxygen would be produced in the requisite quantities, allowing local oxygen to build up in aqueous environments. Therefore, if we find a clear signal for appreciable Mn oxidation in the sedimentary rock record, oxygenic photosynthesis is likely to have evolved by that time.

There are large Mo isotope fractionations, approximately -2.7‰ in δ⁹⁸Mo, associated with the sorption of Mo (as a polymolybdate complex) onto Mn oxyhydroxides (for example, birnessite, vernadite; Fig. 1a; refs 16,17). In contrast, sorption of Mo onto the Fe oxyhydroxide (for example, ferrihydrite) results in a fractionation of only -1.1‰ (Fig. 1a) or less¹⁸. Therefore, if Mn oxidation occurred during sediment deposition it would be an important vector of Mo transfer to the sediment, and, owing to the large associated Mo isotope fractionation, Mo isotope values should become lighter with increasing Mn content, relative to Fe content. In other words, we suggest that a positive correlation between Fe/Mn ratios and Mo isotope values in chemical sediments

¹Yale University, New Haven, Connecticut 06520, USA, ²IFREMER, Plouzané 56470, France, ³University of Johannesburg, Johannesburg 2092, South Africa, ⁴California Institute of Technology, Pasadena, California 91125, USA, ⁵Institut Universitaire Européen de la Mer, Plouzané 29280, France, ⁶Lawrence University, Appleton, Wisconsin 54911, USA, ⁷University of Illinois, Urbana-Champaign, Illinois 61820, USA, ⁸University of Alberta, Edmonton, Alberta T6G 2R3, Canada, ⁹University of California, Riverside, California 92521, USA. *e-mail: noah.planavsky@yale.edu

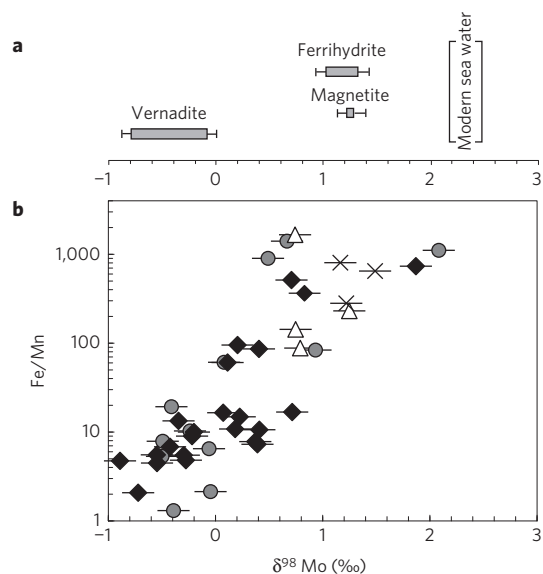


Figure 1 | Evidence for Mn oxidation in Precambrian iron formations.

a, Characteristic Mo isotope fractionations during sorption to oxide mineral surfaces, highlighting the larger Mo isotope fractionations associated with Mo sorption onto Mn oxides relative to Fe oxides (note that the seawater value is modern sea water^{16–18}). **b**, The strong positive correlation between Mo isotope values and the amount of Fe relative to Mn in the ~2.95 Myr old (Ma) Sinqeni Formation (and slightly younger Parktown Formation; diamond), the ~2,700 Ma Manjeri iron formation (triangle), the ~2,320 Ma Timeball Hill ironstone (cross) and the 1,880 Ma Animikie Basin iron formations (circle). The apparent inverse correlation between Mn oxide content and $\delta^{98}\text{Mo}$ values suggests that Mn oxidation was a vector of Mo transfer to the sediment during deposition of the Sinqeni Formation. Error bars based on full protocol duplicates (Supplementary Information).

(for example, iron formations or carbonates) provides compelling evidence for Mn oxidation in the environment. The water column underneath the zone of Mn oxidation needs to be free of sulphide and ferrous Fe for Mn- oxyhydroxide-bound Mo to be shuttled to sediments, given that these species are efficient reductants for Mn oxyhydroxide phases. As molybdate should be the stable Mo species even at prebiotic oxygen levels and small amounts of Mo are likely to be sourced to the oceans regardless of atmospheric $p\text{O}_2$ (ref. 19), this approach can be used to track the presence of local marine

oxygen oases. Furthermore, this Mo isotope approach should hold regardless of the original isotopic composition of sea water.

We find a strong positive correlation between $\delta^{98}\text{Mo}$ values and Fe/Mn ratios in iron formations deposited before and after the GOE. Most strikingly, Mo isotope values and Fe/Mn ratios correlate over a 2.5‰ range in $\delta^{98}\text{Mo}$ values (Fig. 1) in the Mn-rich (0.1–6 wt%) iron formation of the 2.95-Gyr-old Sinqeni Formation, South Africa³. The large isotopic shifts occur over a relatively thin (3-m-thick) horizon (see Supplementary Information for details on the geological setting). We propose this relationship is best explained by short-term variations in the degree of Mn oxidation that are consistent with localized O_2 generation and rapid consumption in a geochemical backdrop that was otherwise reducing. The observed range in $\delta^{98}\text{Mo}$ values and the correlation between $\delta^{98}\text{Mo}$ values and Fe/Mn ratios is statistically identical (Supplementary Information) to that found in the ~1.89-Gyr-old iron formations from the Lake Superior region, Animikie Basin²⁰, which were deposited well after the rise of atmospheric oxygen.

We find this signal for Mn(II) oxidation even though the Mn in the Sinqeni Formation is present in reduced (Mn^{2+}) forms (Fig. 2)—associated with carbonate minerals and to a lesser extent spessartine, a Mn-rich garnet (Supplementary Information). This mineralogical association points to retention of $\delta^{98}\text{Mo}$ signatures for Mn oxidation despite subsequent reduction of the Mn host within the sediment pile. Given that the examined sections of the Sinqeni iron formation are extremely sulphide-poor, the Mo delivered to the sediments with Mn oxyhydroxides is likely to have been trapped in early diagenetic mineral phases (for example, diagenetic carbonates). *In situ* mineral analysis confirms that Mo is found in the carbonate fraction (Supplementary Fig. 5).

The large observed range of Mo isotope values is not easily tied to progressive removal of light Mo onto Fe oxyhydroxides in an upwelling water mass. This process should lead to a negative correlation between Mo and Fe isotope values due to the progressive sequestration of isotopically heavy Fe and light Mo isotopes with precipitating Fe oxyhydroxides²¹. A negative Mo and Fe isotope correlation would develop in an Fe-rich chemical sediment even if there was a switch from partial to quantitative Fe oxidation. In our samples from the Sinqeni Formation there is a weak (though non-significant), positive correlation between $\delta^{98}\text{Mo}$ and $\delta^{56}\text{Fe}$ values (Supplementary Information). Thus, coupled Mo and Fe isotope systematics seem to exclude the possibility that the observed Mo isotope variability in the Sinqeni Formation is tied to a distillation process and amplification of small Mo isotope fractionations.

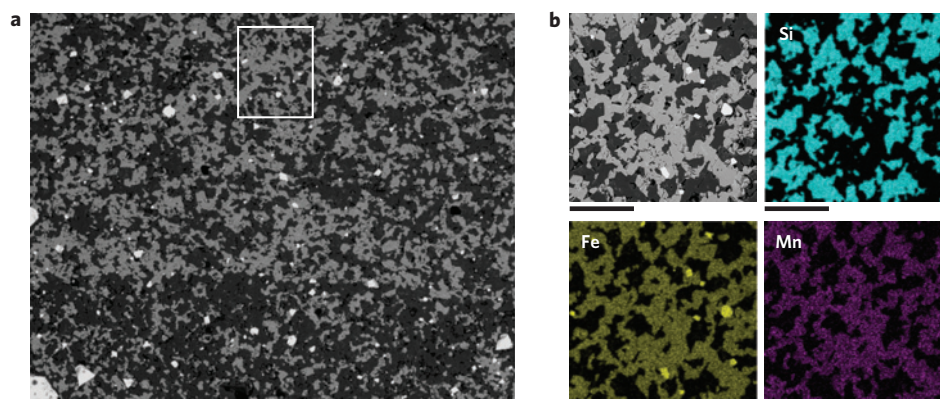


Figure 2 | Backscattered electron images and energy-dispersive X-ray spectroscopy major element maps of a representative Mn-rich ([Mn] = 5.8%) sample from the Sinqeni iron formation (TSB07-26-165.42). **a, b**, The Mn is present in Fe–Mn carbonates (light grey) in a matrix of microcrystalline quartz (dark grey). The Fe–Mn carbonates are associated with euhedral magnetite grains (white grains). The Mo isotope signature of oxidative processes is found in rocks dominated by reduced mineral phases, suggesting that the isotopic signal is not tied to late-stage supergene alteration. Scale bars, 500 μm (**a**) and 100 μm (**b**). See Supplementary Information for additional petrography.

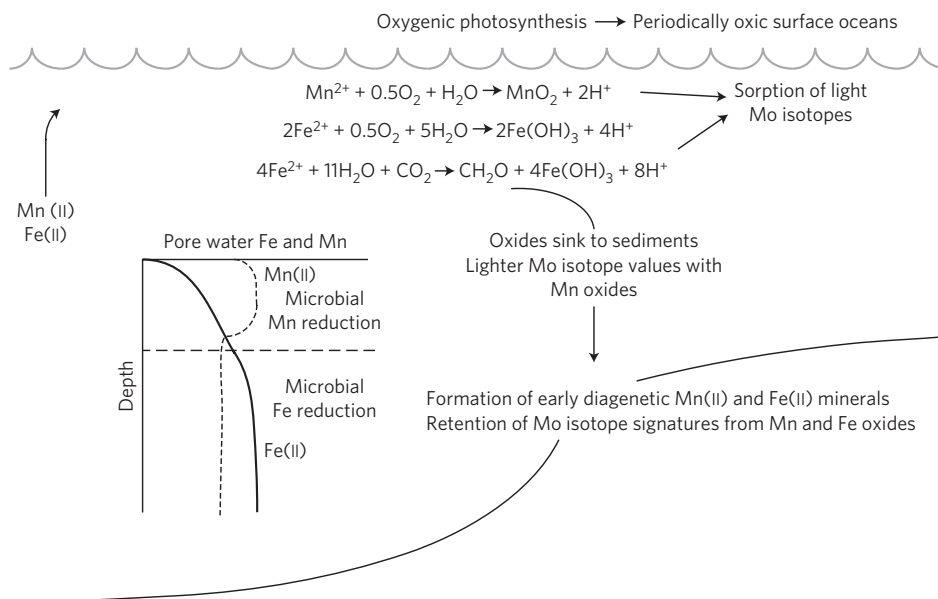


Figure 3 | Overview of the presented model for Mn-Fe-Mo cycling during deposition of the 2.95-Gyr-old Sinqeni iron formation. Sediment Mo isotope variability is tied to Mo being brought to the sediment pile with either Fe or Mn oxyhydroxides. Sediments record the isotopic composition of Mo shuttled to the sediment-water interface by metal oxides.

Furthermore, Mo sorption to iron oxyhydroxides does not provide an explanation for the observed correlation between $\delta^{98}\text{Mo}$ values and Fe/Mn ratios, which is easily explained by a Mn oxide flux to the sediment-water interface.

The mineral assemblage and post-depositional history of the Sinqeni iron formation provide additional constraints on the origin of the observed Mn enrichments. The dominance of reduced Mn and Fe mineral phases strongly suggests that the strong Mn enrichments are not linked to postdepositional supergene alteration, which is probably the case for some Mn-rich Mesoarchaeon units (for example, the ~ 2.75 -Gyr-old Paint Rock member of the Steep Rock Group²²). The Sinqeni Formation in sampled drillcore and outcrop sections of the White Mfolozi Inlier has experienced greenschist facies metamorphism, with peak metamorphism before 2.6 Ga (refs 23,24). Moreover, the Pongola Supergroup is intruded by undeformed post-Pongola granites, which typically fall in the age range between 2.8 and 2.7 Gyr (ref. 3). In the iron formations, the most significant mineralogical change during this peak metamorphism was the formation of coarse-grained magnetite and ankerite and the Mn-rich garnet spessartine (Supplementary Information). In more highly metamorphosed sections of the Sinqeni Formation in southern Swaziland, essentially all of the Mn is present as spessartine²⁵. Spessartine is a common metamorphic product in sedimentary Mn-rich rocks, but its presence in the Sinqeni Formation is significant as peak metamorphism before about 2.6 Ga (ref. 24) firmly places the observed Mn enrichment and thus the associated Mo isotope effect as Archaean in origin. Thus, fairly straightforward geologic and mineralogical constraints provide strong evidence that the Sinqeni Formation preserves a primary signal for Mn oxidation (and thus local free O_2) that is Mesoarchaeon in age and is most readily attributed to syndepositional processes 2.95 Ga.

We suggest that these new Mo isotope data from the Sinqeni Formation, attesting as they do to the antiquity of Mn oxidation (Fig. 3), provide a new and robust minimum estimate for biological oxygen production that pre-dates the most popular estimates by roughly 300–500 Myr (ref. 5). The iron formations of the Sinqeni Formation were deposited in a broad epicontinental sea²⁶. There would have been a limited supply of reductants sourced from deep

waters (for example, methane, ammonium, ferrous iron) to this depositional setting, allowing for local (and perhaps anomalous) oxygen accumulation to levels supporting Mn oxidation even beneath an oxygen-poor atmosphere. This model is consistent with previous interpretations of light iron isotope values in the Sinqeni Formation (Supplementary Information) that linked negative $\delta^{56}\text{Fe}$ values to drawdown of the ferrous iron reservoir²⁷ or to a microbially recycled, benthic iron flux²⁸.

Until recently, organic biomarkers have been the main tool used to track early biological evolution and were essential in establishing the paradigm that oxygenic photosynthesizers appeared by at least 2.7 Ga (ref. 29). This early biomarker work has shaped our view of Precambrian biological evolution and has been central in establishing the idea that the Earth's atmosphere was essentially anoxic for hundreds of millions of years after the emergence of oxygenic photosynthesis¹. However, conclusions drawn based on previous biomarker data are now challenged with increasing vigour (for example, ref. 4). In parallel with growing concerns about the integrity of the Archaean biomarker record, there has been a resurgence of models linking the rise of atmospheric oxygen directly to the first appearance of oxygenic photosynthesis^{4,8,30}. This shift in paradigm contrasts with the emerging record of molecular evolution. New phylogenomic approaches exploring the collective record of the evolution of gene families and protein domain structures point towards a rapid diversification of aerobic enzymes—and by inference an aerobic biosphere, at least locally—between ~ 3.1 and ~ 2.85 Ga (ref. 31). Our study and other recent geochemical work on the Pongola Supergroup³² reconcile geochemical and molecular records for the emergence of oxygenic photosynthesis and provides strong evidence that there was biological oxygen production well before its permanent accumulation in the atmosphere around 2.5–2.3 Ga.

Methods

For Mo and Fe isotope analyses acid digest splits were doped with a Mo double spike and chromatographically separated. After spike addition, element separation was achieved using a two-stage column procedure. Mo and Fe isotope compositions were analysed using a Thermo Neptune MC-ICP-MS instrument at the Pôle Spectrométrie Océan, IFREMER Brest (France). Error, based on

duplicate analysis, is at 2σ level $< 0.15\%$ (see Supplementary Information for full methods)

Received 24 January 2014; accepted 19 February 2014;
published online 23 March 2014

References

- Farquhar, J., Zerkle, A. L. & Bekker, A. Geological constraints on the origin of oxygenic photosynthesis. *Photosynth. Res.* **107**, 11–36 (2011).
- Holland, H. D. The oxygenation of the atmosphere and oceans. *Phil. Trans. R. Soc. B* **361**, 903–915 (2006).
- Mukasa, S. B., Wilson, A. H. & Young, K. R. Geochronological constraints on the magmatic and tectonic development of the Pongola Supergroup (Central Region), South Africa. *Precamb. Res.* **224**, 268–286 (2013).
- Rasmussen, B., Fletcher, I. R., Brocks, J. J. & Kilburn, M. R. Reassessing the first appearance of eukaryotes and cyanobacteria. *Nature* **455**, 1101–1103 (2008).
- Buick, R. When did oxygenic photosynthesis evolve? *Phil. Trans. R. Soc. B* **363**, 2731–2743 (2008).
- Rosing, M. T. & Frei, R. U-rich Archaean sea-floor sediments from Greenland: Indications of 3,700 Ma oxygenic photosynthesis. *Earth Planet. Sci. Lett.* **217**, 237–244 (2004).
- Kirschvink, J. L. & Kopp, R. E. Paleoproterozoic icehouses and the evolution of oxygen mediating enzymes: The case for a late origin of photosystem-II. *Phil. Trans. R. Soc. B* **363**, 2755–2765 (2008).
- Kopp, R. E., Kirschvink, J. L., Hilburn, I. A. & Nash, C. Z. The paleoproterozoic snowball Earth: A climate disaster triggered by the evolution of oxygenic photosynthesis. *Proc. Natl Acad. Sci. USA* **102**, 11131–11136 (2005).
- Rashby, S. E., Sessions, A. L., Summons, R. E. & Newman, D. K. Biosynthesis of 2-methylbacteriohopanepolyols by an anoxygenic phototroph. *Proc. Natl Acad. Sci. USA* **104**, 99–104 (2007).
- Diem, D. & Stumm, W. Is dissolved Mn(II) being oxidized by O₂ in absence of Mn-bacteria or surface catalysts. *Geochim. Cosmochim. Acta* **48**, 1571–1573 (1984).
- Tebo, B. M., Johnson, H. A., McCarthy, J. K. & Templeton, A. S. Geomicrobiology of manganese(II) oxidation. *Trends Microbiol.* **13**, 421–428 (2005).
- Hansel, C. M., Zeiner, C. A., Santelli, C. M. & Webb, S. M. Mn(II) oxidation by an ascomycete fungus is linked to superoxide production during asexual reproduction. *Proc. Natl Acad. Sci. USA* **109**, 12621–12625 (2012).
- Learman, D., Voelker, B., Vazquez-Rodriguez, A. & Hansel, C. Formation of manganese oxides by bacterially generated superoxide. *Nature Geosci.* **4**, 95–98 (2011).
- Clement, B. G., Luther, G. W. & Tebo, B. M. Rapid, oxygen-dependent microbial Mn(II) oxidation kinetics at sub-micromolar oxygen concentrations in the Black Sea suboxic zone. *Geochim. Cosmochim. Acta* **73**, 1878–1889 (2009).
- Anbar, A. D. & Holland, H. D. The photochemistry of manganese and the origin of banded iron formations. *Geochim. Cosmochim. Acta* **56**, 2595–2603 (1992).
- Barling, J. & Anbar, A. D. Molybdenum isotope fractionation during adsorption by manganese oxides. *Earth Planet. Sci. Lett.* **217**, 315–329 (2004).
- Wasylenki, L. E., Rolfe, B. A., Weeks, C. L., Spiro, T. G. & Anbar, A. D. Experimental investigation of the effects of temperature and ionic strength on Mo isotope fractionation during adsorption to manganese oxides. *Geochim. Cosmochim. Acta* **72**, 5997–6005 (2008).
- Goldberg, T., Archer, C., Vance, D. & Poulton, S. W. Mo isotope fractionation during adsorption to Fe (oxyhydr)oxides. *Geochim. Cosmochim. Acta* **73**, 6502–6516 (2009).
- Sverjensky, D. A. & Lee, N. The great oxidation event and mineral diversification. *Elements* **6**, 31–36 (2010).
- Fralick, P., Davis, D. W. & Kissin, S. A. The age of the Gunflint Formation, Ontario, Canada: Single zircon U–Pb age determinations from reworked volcanic ash. *Can. J. Earth Sci.* **39**, 1085–1091 (2002).
- Czaja, A. D. *et al.* Evidence for free oxygen in the Neoproterozoic ocean based on coupled iron-molybdenum isotope fractionation. *Geochim. Cosmochim. Acta* **86**, 118–137 (2012).
- Machado, A. B. On the origin and age of the Steep Rock buckshot, Ontario, Canada. *Chem. Geol.* **60**, 337–349 (1987).
- Hammerbeck, E. C. I. *The Usushwana Complex in the Southeastern Transvaal with Special References to its Economic Potential* Ph.D. thesis, Univ. Pretoria (1977).
- Elworthy, T., Eglinton, B. M., Armstrong, R. A. & Moyes, A. B. Rb–Sr isotope constraints on the timing of late to post-Archaean tectonometamorphism affecting the southeastern Kaapvaal Craton. *J. Afr. Earth Sci.* **30**, 641–650 (2000).
- Horváth, P., Reinhardt, J., Hofmann, A. & Nagy, G. High-grade metamorphism of ironstones in the Mesoarchaean of southwest Swaziland. *Mineral. Petrol.* <http://dx.doi.org/10.1007/s00710-013-0307-1> (2014).
- Beukes, N. J. & Cairncross, B. A Lithostratigraphic–sedimentological reference profile for the Late Archaean Mozaan Group, Pongola Sequence: Application to sequence stratigraphy and correlation with the Witwatersrand Supergroup. *S. Afr. J. Geol.* **94**, 44–69 (1991).
- Planavsky, N. *et al.* Iron isotope composition of some Archean and Proterozoic iron formations. *Geochim. Cosmochim. Acta* **80**, 158–169 (2012).
- Johnson, C. M., Beard, B. L., Klein, C., Beukes, N. J. & Roden, E. E. Iron isotopes constrain biologic and abiologic processes in banded iron formation genesis. *Geochim. Cosmochim. Acta* **72**, 151–169 (2008).
- Brocks, J. J., Logan, G. A., Buick, R. & Summons, R. E. Archean molecular fossils and the early rise of eukaryotes. *Science* **285**, 1033–1036 (1999).
- Johnson, J. *et al.* Manganese-oxidizing photosynthesis before the rise of cyanobacteria. *Proc. Natl Acad. Sci. USA* **110**, 11238–11243 (2013).
- David, L. A. & Alm, E. J. Rapid evolutionary innovation during an Archaean genetic expansion. *Nature* **469**, 93–96 (2011).
- Crowe, S. *et al.* Atmospheric oxygenation three billion years ago. *Nature* **501**, 535–538 (2013).

Acknowledgements

N.J.P. acknowledges financial support from NSF EAR-PF; O.J.R. and D.A. from Europol Mer and ANR-10-LABX-19-01; A.H. and F.O.O. from the NRF of South Africa and Acclaim Exploration; S.V.L. from NSERC-PF and LabexMer-PF; K.O.K. from NSERC; N.J.P., T.W.L., C.T.R. and T.M.J. from NASA Exobiology; and T.W.L. from NSF EAR. C. Delvigne, J. Hancox and N. Hicks provided access to drill core and samples; E. Ponzevera and Y. Germain provided technical assistance.

Author contributions

N.J.P. wrote the paper with input from all authors. N.J.P., D.A., O.J.R., A.K., S.V.L., F.O.O., E.P., X.W. and C.T.R. generated data. A.H. and N.J.P. provided samples. N.J.P. and C.T.R. designed the study with input from all authors.

Additional information

Supplementary information is available in the [online version of the paper](#). Reprints and permissions information is available online at www.nature.com/reprints. Correspondence and requests for materials should be addressed to N.J.P.

Competing financial interests

The authors declare no competing financial interests.